Available online at www.sciencedirect.com
ScienceDirect
Journal of Nuclear Materials 363–365 (2007) 797–800
journal of nuclear materials
www.elsevier.com/locate/jnucmat

Simulation of charge exchange neutrals interactions with gaps in first wall cladding

V.A. Kurnaev *, D.I. Matveev, N.N. Trifonov

Moscow Engineering and Physics Institute, Kashirskoe sh. 31, 115409 Moscow, Russia

Abstract

Angular distributions of particles impinging PFC in fusion devices with magnetic confinement are briefly discussed. It is shown that simulation of charge exchange neutrals interaction with the first wall should be made for inclined incidence of particles. Particle reflection coefficients and sputtering yields for gaps in Be, C and W first wall cladding are found with Monte Carlo computer simulations for hydrogen isotopes in the energy range $\sim 5–5 \times 10^3$ eV as well as for the flux integrated over the ITER charge exchange neutrals energy spectrum. Trapping of deuterons by the gap in the W wall increases two times (up to ~ 0.6) as compared with the flat surface, while trapping in the Be gap is close to unity. The influence of isotope mass on trapping and sputtering is shown to follow data for the flat surface. Roughness of gap sidewalls taken into account slightly contributes to calculated data.

PACS: 52.40.Hf; 52.25.Yc

Keywords: First wall; Neutrals; Recycling; Sputtering yield; TRIM

1. Introduction

The fuel recycling and tritium retention in fusion devices are of great importance for reactor performance. Many models, describing plasma particles interaction with plasma facing components (PFC) as well as direct measurements are known [1]. But gaps between PFC elements became the subject of consideration only recently. The main problem is the accumulation of tritium in the gaps and first measurements were recently carried out [2–4]. The deposition rate was evaluated to be $(2–5) \times 10^{-4}$ of incoming ion flux, but retained amount of fuel can be ~ 0.3 [4]. The main sources of hydrogen buildup in gaps are the hydrocarbon transport and codeposition. Calculations of hydrogen accumulation in gaps and its subsequent release need a model considering surface temperature and chemistry and adequate description of plasma particles interaction with gap sidewalls.

In our calculations, we did not take into account hydrogen accumulation in gaps due to hydrocarbon transport or codeposition and, as a first step, considered only kinetic effects – reflection and sputtering under impinging hydrogen charge exchange fluxes.

* Corresponding author.
E-mail address: kurnaev@plasma.mephi.ru (V.A. Kurnaev).

0022-3115/$ - see front matter © 2007 Elsevier B.V. All rights reserved.
doi:10.1016/j.jnucmat.2007.01.102

2. Distributions of impinging particles

First wall PFC are bombarded both with charge exchange neutrals and ions drifting (or transporting due to microturbulences) perpendicular to the magnetic field lines across the scrape-off layer (SOL). Energy distributions of fast charge exchange (cx) neutrals are measured practically at all tokamaks during standard ion temperature profile diagnostics with gas or thin film stripping of neutrals to ions and consequent analysis in electrostatic and magnetic analyzers. The time of flight technique is used for low energy part of the charge exchange energy distribution. So, the total energy distributions of neutrals escaping plasma are known for operating devices and are predicted for ITER [5]. But angular distributions $J(\theta_0)$ of cx neutrals striking the PFC surface are not well known. Earlier [6], analytical calculations of $J(\theta_0)$ were carried out for the neutrals emitted by a cylindrical plasma column of radius r_0 with axial magnetic field due to charge exchange of plasma ions of the density $n_i(r)$ with cold neutral atoms of the density $n_a(r)$. The angular distribution of cx neutrals impinging point M on the cylinder surface in the plane perpendicular to the magnetic field was calculated in accordance with

$$J(\theta_0) = \int_{S(\theta_0)} n_i(r) \cdot n_a(r) \langle \sigma_{cx} v \rangle \frac{\cos\varphi}{r'} \mathrm{d}S, \qquad (1)$$

where $S(\theta_0)$ is the surface situated from M at the distance equal to the cx neutral free path λ, r' and φ are radius vector and polar angle of an arbitrary plasma point within distance λ seen from the point M, respectively. Integration of (1) for the simple assumptions $n_a(r) = \exp\{-(r_0 - r)/a\}$ (a is the neutral atoms decay length), $\sigma_{cx} = \text{const}$, $n_i(r) = \text{const}$, ion temperature $T_i(r) = \text{const}$ gave a strong dependence of the most probable angle of incidence θ_m on the relative value of the neutral free path with $\theta_m \neq 0$. Moreover, the finite value of Larmor radius ρ_i in the case of rapid decrease of the neutral atoms density near the wall resulted in asymmetry (relative to the normal to surface) of angular distribution of particles impinging the wall from different plasma areas. To obtain the spatial distribution of impinging neutrals achieving some point on the wall also from other directions, it is necessary to replace $(\cos\varphi)$ in (1) by $(\cos\varphi \cdot \sin\varphi)$ [5], as well, to consider r to be a spatial radius vector. Estimations of θ_m value under simple assumptions about the density and temperature distributions $n = n_0[1 - (r/r_0)^2]$, $T = T_0[1 - (r/r_0)^2]$ for L regime and $n = n_0$, $T = T_0$ at $0 < r/r_0 < (r_{th}/r_0)$, $n = n_0[1 - (r/r_0 - r_{th}/r_0)/(1 - r_{th}/r_0)]$, $T = T_0[1 - (r/r_0 - r_{th}/r_0)/(1 - r_{th}/r_0)]$ at $r_{th}/r_0 \leqslant r/r_0 \leqslant 1$ for H regime, and with the temperature dependence of charge exchange rate taken $\langle \sigma_{cx} v \rangle$ $(\mathrm{m^3\,c^{-1}}) \approx 2.5 \times 10^{-14} \lg T(\mathrm{eV})$ $(10\,\mathrm{eV} < T < 10^4\,\mathrm{eV})$ show that the most probable angle of incidence θ_m can vary in the range of 50–70°.

The contribution of SOL to the first wall loading with ions, depending on conditions, can be estimated to be in the range from a few to 50% of the flux penetrating through the separatrix. Due to estimates for ITER outer mid-plane, cx neutral flux exceeds the ion flux. But the ion flux exceeds the flux of cx neutrals several times at baffle region near the divertor target. Achieving the wall, ions are accelerated by the sheath potential drop $\sim(3–5)T_e$ resulting in straightening of magnetized ions helical trajectories. The most probable angle θ_m of incidence of the ion onto the surface depends on the ratio of the gyro radius to the sheath length. Simple estimations performed for the case the magnetic field of ~3 T crossing PFC surface at small sliding angles $\alpha \sim 3–5°$ for the ion temperature $T_i \sim 20$ eV show that the most probable angle of ion incidence increases from $\theta_m \approx 0$ at $n_e \sim 10^{21}\,\mathrm{m^{-3}}$ to $\theta_m \approx 40°$ at $n_e \sim 10^{18}\,\mathrm{m^{-3}}$ and further up to $\theta_m \approx 90^0 - \alpha$ for very low densities ($\sim 10^{15}$–$10^{16}\,\mathrm{m^{-3}}$). The most probable angle of incidence for the spatial distribution of ions bombarding any point on the PFC surface from all directions, as in the case of cx neutrals, is larger. Summarizing the brief consideration of possible angular distributions of particles impinging PFC, one can conclude that for charge exchange neutrals bombarding first wall cladding with gaps it is of importance to consider the case of sliding incidence of particles.

Turbulent transport in the periphery region can change the angular distribution, but ions accelerated in the very thin sheath layers strike PFC about the normal to the surface. Angular distributions of impinging particles during transient events and ELMs when high-energy ions can bombard PFC are also not known. As the gap width Δ is much larger than Debye radius r_D, periphery plasma penetrates into the gaps and can also contribute to the ion irradiation of gap sidewalls. The ITER first wall cladding has gaps with $\Delta \approx 1$ cm and plasma penetrates into gaps for typical sheath length $\sim 10^{-2}$ cm. In our calculations we do not consider possible contribution of plasma inside the gap on particles trapping and sputtering.

3. Results of simulations and discussion

For simulations, we used code SCATTER [7] based on the binary collision approximation like TRIM but modified to include surface roughness [8]. The applicability of binary collision approximation for hydrogen ions with eV energies for high-Z materials was proved earlier [9]. The gaps with the width Δ are considered to be infinite both in depth and length. Particle reflection coefficient R_N for the gap defined as the ratio of flux backscattered into plasma from the gap area to the incoming flux to this area. Similarly, the sputtering coefficient Y for the gap is the ratio of sputtered PFC atoms flux entering SOL to the incoming flux. For every impinging particle striking the gap side, the trajectory of projectile in sidewall material is calculated. These projectiles, due to collisions with sidewall atoms can be either captured or reflected back into the gap. Also they cause sputtering. Reflected projectiles, in turn, can strike the opposite side of the gap wall resulting in the same processes. The calculations continue till the primary particle entered the gap will be captured by walls or reflected back into plasma. Variable parameters of the primary flux are the energy distribution of incoming hydrogen isotopes and its masses (H, D or T). Energy interval of impinging projectiles is equal to $0.005\,\text{keV} \leqslant E \leqslant 5.0\,\text{keV}$. Tungsten, carbon and beryllium are considered to be the first wall materials, as well, both ideally smooth and rough gap sidewalls surfaces are considered. Surface roughness is simulated with regular triangular ridges of the μm size oriented perpendicular or parallel to the gap entrance. The relief of this kind is typical for the mechanical treatment of the material and influences the hydrogen ions reflection from the surface most of all [10]. The gap width is much larger than microrelief dimensions as well as the most probable free path of projectile in matter. Gap backscattering coefficients R_N and gap sputtering coefficients Y are calculated as functions of the primary energy of impinging particles E incident at $\theta_m = 70°$ on the first wall in the plane perpendicular to the gap edge.

Fig. 1 demonstrates the difference between reflection from the flat plasma facing wall and a gap. R_N decrease for Be gap is higher (4.5 times at energy $E \sim 20$ eV and 10 times at $E = 500$ eV) as compared with W gap (R_N decreases 2 times). The reason is in a worse reflectivity of low-Z sidewalls and, as a result, in smaller probability for particle to escape the gap. Trapping of deuterium by the gap equals

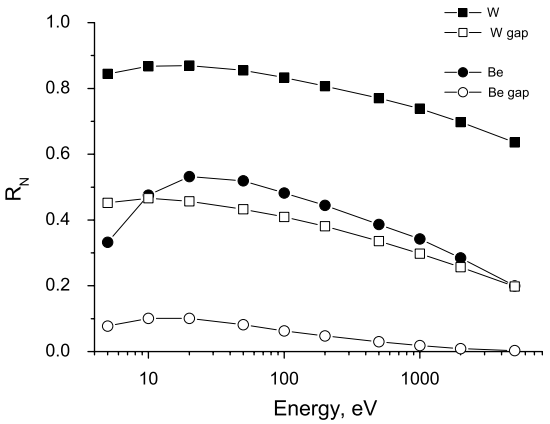

Fig. 1. Particle reflection coefficient as function of primary energy of deuterons impinging W and Be first walls and gaps in its for angle of incidence equal to 70°.

to $1 - R_N$. At the energies less than 100 eV, trapping in the W gap increases more than 3 times from ~15% till ~55% as compared with the flat surface. More than 95% of impinging particles are trapped by Be gap at $E > 100$ eV. The backscattered flux becomes negligible for $E > 1$ keV.

Total values of R_N and Y integrated over the energy of cx neutrals are summarized in Table 1. The energy spectrum of cx neutrals for the outside mid-plane of ITER [5] is used in calculations. One can see that the decrease of reflection from gaps as compared with flat surfaces is more pronounced for low-Z materials. The gap contribution to hydrogen recycling is rather high ($R_N \sim 0.4$) for W. Calculations show that normal incidence of 40–60 eV D^+ ions on the first wall corresponds to $R_N \sim 0.8$ and $R_N \sim 0.35$ for W and Be first wall, respectively. These values are very close to these calculated for cx neutrals at sliding incidence (see Table 1), so, one can expect that the averaged contribution of reflection to hydrogen recycling per impinging particle will be equal for cx neutrals and SOL ions in ITER-like plasma.

Table 1
Integrated over energy of impinging charge exchange deuterium neutrals values of R_N and Y for a first wall with gaps (angle of incidence 70°) with smooth gap sidewalls, with sidewall microrelief ridges perpendicular to the gap depth direction (⊥) and with microrelief ridges parallel to the gap depth direction (‖)

Coefficient	R_N			Y		
Material	Be	C	W	Be	C	W
Wall	0.420	0.480	0.79	0.250	0.087	0.0051
Gap, smooth	0.047	0.063	0.37	0.014	0.004	0.0010
Gap, ⊥	0.060	0.091	0.40	0.021	0.007	0.0012
Gap, ‖	0.057	0.081	0.34	0.025	0.008	0.0011

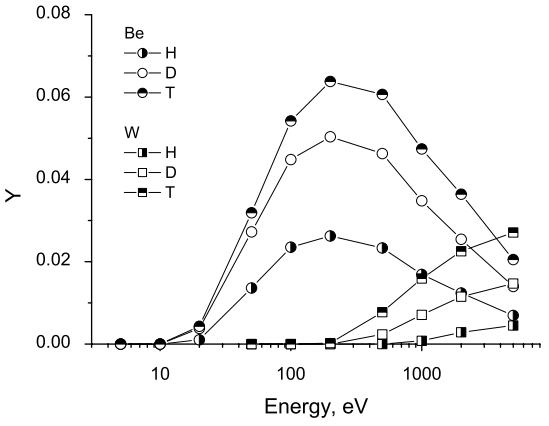

Fig. 2. Sputtering yield as a function of the primary energy of different hydrogen isotopes for the gap in W and Be first wall for the angle of incidence of 70°.

The influence of gaps on plasma contamination due to sputtering of wall atoms is small but not negligible. The flux of the sputtered atoms escaping the gap decreases approximately 5 times as compared with the flat wall. As one can expect, roughness of the gap sidewall increases backscattering and sputtering (it is evident only for light PFC elements) but the total effect is small nevertheless. Calculations for 50 eV D^+ ions at normal incidence on the flat wall corresponding to the SOL ion irradiation show that the sputtering yield for Be is of about 0.01. So, at equal fluxes, contribution of *cx* neutrals to the Be first wall erosion is ~25 times larger than for SOL ions. These estimations of Y for *cx* neutrals are made only for smooth surfaces.

Simulations performed with different hydrogen isotopes exhibit the same R_N and Y dependence on the ion mass both for the flat target and that with gaps, the heavier ion, the higher Y (Fig. 2). As for the reflection, R_N decreases with the ion mass.

Simulations also allowed to find distributions of impinging particles captured in the sidewalls as well as distributions of redeposited material over the gap depth.

4. Summary and conclusion

Consideration of angular distributions of particles escaping hot magnetized plasma shows predominantly inclined incidence of charge exchange neutrals on PFC (with the angle of incidence ~50–70° depending on plasma parameters) as well as SOL ions (at low plasma densities). This results in enhanced hydrogen recycling and wall sputtering.

Particle reflection coefficients R_N and physical sputtering yields Y are calculated for the gaps in Be, C and W first wall cladding bombarded with hydrogen isotopes at the angle of incidence of 70° and energy of $5–5 \times 10^3$ eV. Values of R_N and Y integrated over the energy spectrum of charge exchange neutrals for ITER outer mid-plane are found. Trapping of particles by gaps depends on atomic number of PFC material increasing for deuterons in W gap 2 times (up to ~0.6) as compared with the flat surface and approaching unity in Be gap. Averaged contribution to hydrogen recycling per impinging particle is estimated to be equal for charge exchange neutrals and SOL ions. Sputtering coefficient of Be first wall under charge exchange neutrals is evaluated to be ~25 times larger than under SOL ions. Trapping and sputtering in gaps increase about proportional to the mass of impinging hydrogen isotope. Roughness of gap sidewalls increases backscattering and sputtering for low-Z gaps, but the total contribution of roughness is insignificant as the reflection and sputtering yields are small.

Acknowledgements

Authors are thankful to A.S. Kukushkin for fruitful discussions. This work was supported by Russian Agency for Atomic Energy under contract 1.05.19.19.06.538. The research described in this publication was made possible in part by Award No. RUX0-013-PZ-06 of the US Civilian Research & Development Foundation (CRDF) and of the Ministry of Education and Science of Russian Federation.

References

[1] P. Stangeby, Plasma Boundary in Fusion Devices, IOP Publishing, 2000.
[2] M. Rubel et al., Phys. Scr. T111 (2004) 112.
[3] M. Brosset et al., Fourth IAEA TM SSO, India, 2005.
[4] A. Litnovsky, V. Phillips, P. Wienhold, et al., J. Nucl. Mater. 337–339 (2005) 917.
[5] R. Behrisch, G. Federici, A. Kukushkin, D. Reiter, J. Nucl. Mater. 313–316 (2003) 388.
[6] M. Gulin, V.A. Kurnaev, S.K. Zhdanov, Phys. Plasma 6 (1983) 461 (in Russian).
[7] N.N. Koborov, V.A. Kurnaev, N.N. Trifonov, et al., Nucl. Instrum. and Meth. B 129 (1997) 5.
[8] V.A. Kurnaev, N.N. Trifonov, Phys. Scr. T103 (2003) 85.
[9] A.A. Evanov, V.A. Kurnaev, D.V. Levchuk, et al., Nucl. Instrum. and Meth. B 135 (1998) 532.
[10] V.V. Bandurko, N.N. Koborov, V.A. Kurnaev, V.M. Sotnikov, J. Nucl. Mater. 176&177 (1990) 630.